A distributed water balance model to estimate direct groundwater recharge: A case study from the Nhoma and Khaudum catchments, Namibia

Heike Wanke[1]*, Armin Dünkeloh[2], Peter Udluft[2], Ansgar Wanke[1]
[1]Department of Geology, University of Namibia
340 Mandume Ndemufayo Avenue, Private Bag 13301, Pioneerspark, Windhoek, Namibia
[2]LFB Hydrogeology and Environment, Institute of Geology, Pleicherwall 1, 97070 Würzburg, Germany

Received: 16th July, 2013. Accepted: 15th October, 2013.

Abstract

The most important water resource in drylands such as Namibia is groundwater and its recharge including temporal and spatial variations need to be assessed reliably for sustainable water management. In this paper, a grid-based conceptual water balance model with a simplification at the catchment scale level is used to assess groundwater recharge. The reliability of the model predictions are verified by the independent chloride mass balance method. The distributed, process-oriented, physically based water balance model MODBIL used in this study considers the major water balance components and calculates a spatially differentiated water balance by simulating water fluxes and storages at temporal and spatial resolutions based on meteorological, topographic, soil physical, land cover and geological input parameters. In this study it is set up for the upper Khaudum and Nhoma catchments in the Kalahari of north-eastern Namibia and northwestern Botswana at a spatial resolution of 500 x 500 m, calculated daily for a period of 22 years. A mean annual area groundwater recharge of 11.5 mm a^{-1} is calculated for the catchments, but spatial variations between 0 and 17.5 mm a^{-1} occur depending on the variability of vegetation, soil and geomorphology. Groundwater recharge only occurred on a few days during the simulation period.

Keywords: Soil water balance model; Namibia; Groundwater recharge; Kalahari; Chloride Mass Balance.

ISTJN 2013; 2(1):11-32.

*Corresponding author - E-mail: hwanke@unam.na

1 Introduction

Groundwater resources in arid areas such as Namibia are much more important than surface water as it easily evaporates and is not reliable especially in dry years. In the study area the groundwater recharge and its temporal and spatial variations need to be assessed reliably in order to manage groundwater resources sustainably and to prevent the over-exploitation of aquifers that may threaten survival. Reviews on groundwater recharge estimation are available in Lerner et al. (1990), Simmers (1997) and Scanlon and Cook (2002). Most of the reliable techniques for groundwater recharge estimations are limited to temporal or spatial point results, but grid-based water balance models with sensible simplification at the catchment scale are the only appropriate tools for long-term water resource planning. Basic demands on such water balance models are the adequate representation of physical processes. Furthermore, models must be set up for a significantly long time span with a high temporal resolution. Daily climatic data, which acknowledge the important significance of single events, are found to be appropriate for recharge estimation in drylands (Hendrickx and Walker 1997). One of the most critical factors is the determination of evapotranspiration. An appropriate and detailed review on estimation of real evapotranspiration is given by Allen et al. (1998). The simulation of groundwater recharge must be based on physical processes in the soil moisture storage and simulated in small time steps, at least daily. A common simplification here is the concept of field capacity, where a soil drains freely once the relevant water content is reached (e.g. Rushton et al. 2006).

However, as precipitation and evapotranspiration in drylands are several orders of magnitude higher then groundwater recharge, verification of the results becomes a major challenge. Thus, other recharge estimation techniques should be an integrated part of water balance modelling. Remote sensing techniques for evapotranspiration estimation (e.g. Brunner et al. 2004) can be used to examine the spatial pattern, hydrographs for the temporal variations (e.g. Külls 2000), or tracer (Gieske 1992; Selaolo 1998) and lysimeter studies for the appropriate point calibration.

So far for the Kalahari in Namibia (in Botswana studies were done by e.g. Beekman et al. 1996; Selaolo et al. 1996), only point recharge data exist (e.g. Wrabel 1999; Stone 2012) or small scale water balance models that integrate groundwater recharge estimations exist (e.g. Külls 2000; Klock 2002). A large scale GIS-based model for the southern African region (Alemawa and Chaoka 2003) simulates only surface run-off and evapotranspiration, and groundwater recharge is not considered at all in their study. A large scale water balance model set up for the Kalahari catchment of north-eastern and North-Western Botswana by Wanke et al. (2008) is only verified by published regional data but not by point data. Thus, the aim of the present study is to show the strength of a complete water balance model for two sub-catchments of the Kalahari and to verify them with independent point data. Temporal variations of groundwater recharge, evapotranspiration and runoff, as well as the spatial pattern of groundwater recharge in a typical setting of spatial varying vegetation and geomorphological regime of the Kalahari, are calculated. Verification of the results is made by the chloride mass balance method

(CMB) and by comparison with groundwater hydrographs. The resulting water balance model is based on a grid cell size of 500 x 500 m for the upper Khaudum and Nhoma catchments in north-eastern Namibia and north-western Botswana for 22 years with a daily resolution.

2 Methodology

2.1 Model formulation

The distributed, GIS-based, process-oriented, physically based water balance model (MODBIL after Udluft and Dünkeloh, 2005) used in this study considers four major water balance components: groundwater recharge, surface runoff, interflow, and evapotranspiration. MODBIL (Udluft and Dünkeloh 2005) calculates a spatially differentiated water balance by simulating water fluxes and storages at temporal and spatial resolutions based on meteorological, topographic, soil physical, land cover and geological input parameters.

The model handles the temporal and spatial variations of the water balance components in two major process steps (Fig. 1). In the first step, meteorological data (precipitation, temperature and relative humidity) are interpolated for each active raster cell depending on topographic parameters (altitude, slope and aspect). A snow-module is driven by precipitation and temperature (not applicable for this case study). Effective precipitation is calculated with respect to the canopy storage capacity (dependent on land cover class).

The second model step simulates storage, evapotranspiration, surface runoff, interflow and groundwater recharge based on soil, subsoil and land cover parameters. A one layer model calculates the soil moisture conditions and the relevant fluxes into and out of the soil system for each time step. Surface runoff and infiltration are calculated depending on effective precipitation, soil hydraulic conductivity and surface hydraulic conductivity. The infiltrating part is added to the soil water storage. Surface runoff/interflow occurs if a) the infiltration amount exceeds the maximum infiltration capacity that is limited by permeability, or b) the soil moisture storage has reached the maximum value (field capacity).

In addition, soil moisture is lost in every time step due to real evapotranspiration. This is calculated using potential evaporation, soil moisture content and vegetation type in a modified method after Renger et al. (1974) and Sponagel (1980). The potential evaporation is calculated using the Penman-Monteith equation (Monteith 1965; Allen et al. 1998). Deep percolation/groundwater recharge starts if soil moisture content exceeds effective field capacity. The amount of groundwater recharge is driven by the amount of water percolation in the soil, and by the hydraulic conductivity of both the soil and the subsoil. Interflow is revealed if the percolation exceeds the maximum permeability of the subsoil.

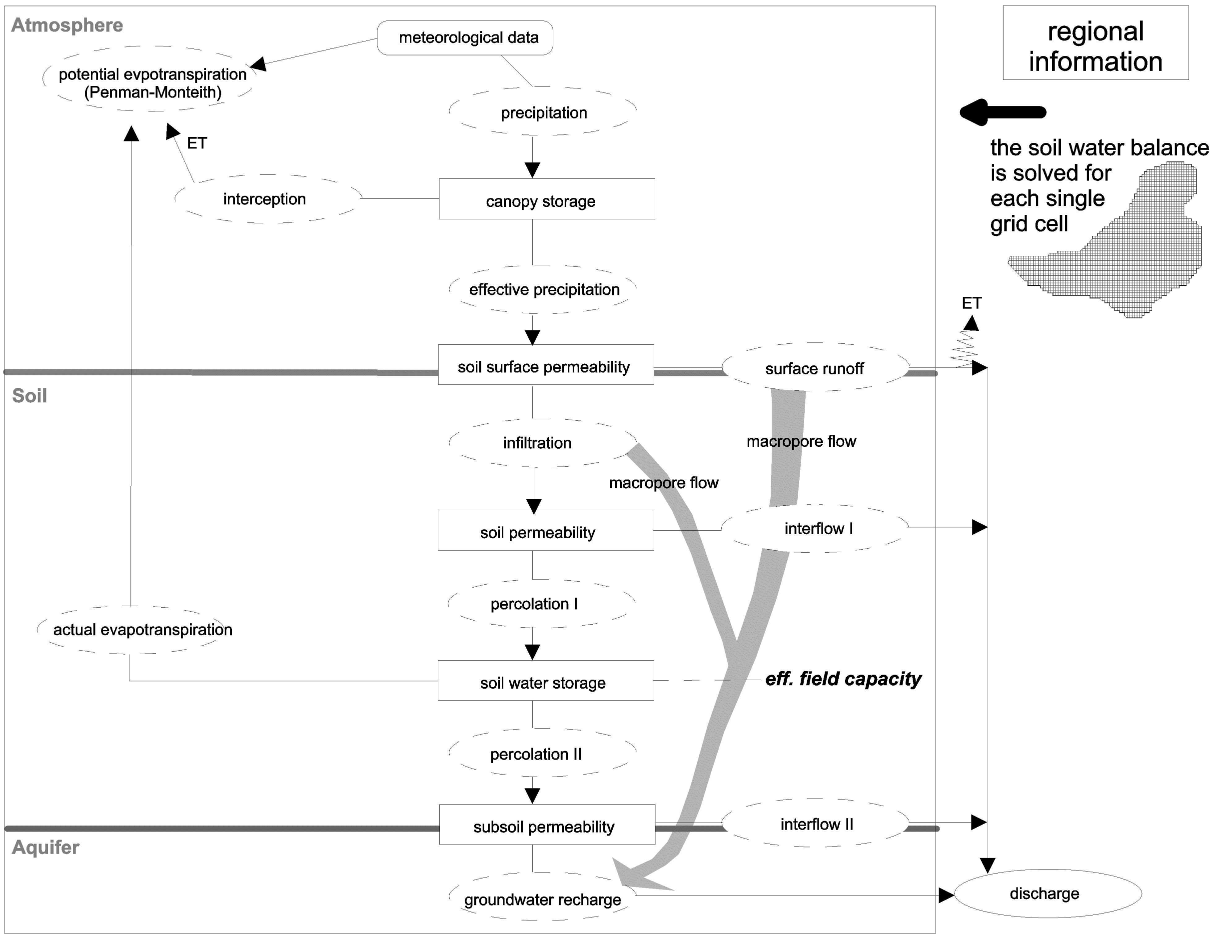

Figure 1: Flow chart representing the water balance model MODBIL (modified after Wanke et al. 2008).

2.2 Regionalisation of meteorological data

Regionalisation of meteorological data requires a compromising selection of the calculation procedure as calculation times and accuracy have to be considered. Therefore a relatively simple approach is chosen in this study. First, the reference altitude (*AR*), daily uncorrected precipitation (*PU*) and uncorrected temperature (*TU*) are calculated by the inverse distance to a power method for each grid cell. In a second step, precipitation (*P*) and temperature (*T*) are corrected for altitude effects assuming a precipitation gradient of 4.4%/100 m and a temperature gradient of 0.65°*C*/100 m, using the reference altitude and the real altitude of the grid cell (*AG*) as given by a digital elevation model (*DEM*):

$$P = PU(1 + [AG - AR] \times 0.00044) \tag{1}$$

$$T = TU(1 + [AG - AR] \times 0.0065) \tag{2}$$

2.3 Calculation of potential evaporation

The calculation of the potential evaporation is based on the Penman-Monteith equation (Monteith 1965) as given by Allen et al. (1998):

$$ET_0 = (0.408\Delta[Rn - G] + \gamma[900/(T + 273)]u_2[e_s - e_a])/(\Delta + \gamma[1 + 0.34u_2]) \tag{3}$$

with:

ET_0	reference evapotranspiration [mm d^{-1}]
Rn	net radiation at the crop surface [MJ m^{-2} d^{-1}]
G	soil heat flux density [MJ m^{-2} d^{-1}]
T	mean daily temperature at 2 m height [°C]
u_2	wind speed at 2 m height [m s^{-1}]
e_s	saturation vapour pressure [kPa]
e_a	actual vapour pressure [kPa]
$e_s - e_a$	saturation vapour pressure deficite [kPa]
Δ	slope vapour pressure curve [kPa °C^{-1}]
γ	psychrometric constant [kPa °C^{-1}]

Day length and radiation are calculated as described in detail by Allen et al. (1998).

2.4 Calculation of effective precipitation

Incoming precipitation is separated into interception, stem flow and through fall when entering the surface vegetation. The latter two are thus summed together as effective precipitation

Table 1: Soil and vegetation parameters for the 6 land cover classes used in the water balance model.

Land unit	Geomorphologic position	Area (%)	Soil type	Water content at field capacity (cm m^{-1})	Water content at wilting point	Residual water content	Plant available water content	Eff. root depth (cm)	Available water content	Eff. k_f at field capacity (m s^{-1})	Interception‡ (mm)	K_C
Mixed Savanna	sand plain	42.81	arenosol, calcisol	168	92	10	158	80	126	1.85E-06	4/0	0.96
Burkea africana Savanna	thick sand plain	45.02	Arenosol	133	66	10	123	80	98	3.30E-06	4/2	0.98
Acacia shrubland	shallow soil, hard pan	10.08	regosol, calcisol	203	118	35	168	80	135	4.00E-07	4/4	0.9
Grassland	dry river beds, pans	0.47	Fluvisol	263	168	50	213	40	85	5.00E-08	1/0	1
Baikiaea plurijuga Woodland	dune crests	0.87	Arenosol	133	66	10	123	100	123	3.30E-06	5/0	0.98
Terminalia prunioides Woodland	hard pans, hardrock ridges	0.75	regosol, calcisol	203	118	35	168	100	168	4.00E-07	2/0	0.98

‡Leaf production has been set from October to April for savannas and woodlands and grass production from December to May according to a phonological study by Chidumayo (2001) and references therein.

(PE). Spatial and temporal variations of total interception storage capacity (IT) used in this model are given per land cover classes (see Table 1). Intercepted precipitation is lost from the storage by evaporation (calculated with ET_0) and the actual interception storage capacity (IA) is adjusted for the next time step. Although only daily precipitation data are available, it is assumed that the largest part of the rain falls within a time constraint of 3 hours as observed during field work. These are summarized as

$$IA_t = IT \qquad P_t > IT - IA_{t-1} \tag{4}$$

$$IA_t = IA_{t-1} + P_t \qquad P_t \leq IT - IA_{t-1} \tag{5}$$

$$IA_{t+1} = IA_t - ET_{0t} \qquad ET_{0t} \leq IA_t \tag{6}$$

$$IA_{t+1} = 0 \qquad ET_{0t} > IA_t \tag{7}$$

In MODBIL, effective precipitation is then calculated as:

$$PE_{t+1} = P_t - IA_t \qquad P_t > IA_t \tag{8}$$

$$PE_{t+1} = 0 \qquad P_t \leq IA_t \tag{9}$$

2.5 Surface runoff, interflow and infiltration

The effective daily precipitation is first separated into direct surface runoff (R) and infiltration (F) depending on the permeability of the soil surface (KS). If the effective precipitation exceeds the permeability of soil surface, surface runoff occurs. Here again the daily effective precipitation is assumed to occur within 3 hours as defined by the algorithm to reflect field observation.

$$F = KS \qquad PE > KS \tag{10}$$
$$R = PE - KS \qquad PE > KS \tag{11}$$
$$F = PE \qquad PE \leq KS \tag{12}$$
$$R = 0 \qquad PE \leq KS \tag{13}$$

The permeability of soil surface depends on the permeability of the soil (KF) and is modified by factors for land cover (LC), terrain slope (TS), and soil water content (SW):

$$KS = KF \times LC \times TS \times SW \tag{14}$$

with:
LC(forests) = 10
LC(grassland, meadow, fields) = 2.5
LC(wetlands) = 5
LC(settled areas) = 0.5
$TS = 1/(1 - \tan(\pi/[180 \times \beta]))$
$SW = 1/(0.2 + 0.008 \times PS)$
where β = slope of the terrain [%]
PS = percentage of saturation, expressed in % of field capacity.

In the next step infiltration is compared with the permeability of the soil itself and is subsequently divided into percolation I (DPI) and interflow I (WI).

$$DPI = KF \qquad F > KF \tag{15}$$
$$WI = F - KF \qquad F > KF \tag{16}$$
$$DPI = F \qquad F \leq KF \tag{17}$$
$$WI = 0 \qquad F \leq KF \tag{18}$$

The percolation then increases the soil water content (see below) and influences the permeability of the soil surface border for the next time step. Two different scenarios of macropore flow were tested during modelling performance: a) the surface runoff can lead to macropore flow (depending on land units) which short cuts directly to groundwater recharge, and b) a fixed portion of the infiltration leads to macropore flow and short cuts to groundwater recharge (grey arrows in Fig. 1). However, both approaches are found not to improve the modelling results in this case study and this process has thus been excluded from the simulation.

2.6 Soil water content

Soil water content (Θ) is increased by infiltration into the soil and reduced due to actual evapotranspiration (ET_A). It can increase up to a maximum of field capacity (FC); further water influx leads to the development of percolation II (*DPII*). Each day is divided into 10 time steps for the calculation of the state of the soil moisture storage, and soil moisture calculates as:

$$\Theta_{t+1} = \Theta_t + DPI_t - ET_{At} \qquad FC > \Theta_{t+1} \tag{19}$$
$$DPII_{t+1} = 0 \qquad FC > \Theta_{t+1} \tag{20}$$
$$\Theta_{t+1} = FC \qquad FC \leq \Theta_{t+1} \tag{21}$$
$$DPII_{t+1} = \Theta_t + DPI_t - ET_{At} - FC \qquad FC \leq \Theta_{t+1} \tag{22}$$

Actual evapotranspiration is controlled by the soil water content as given in the next section (2.7).

2.7 Actual Evapotranspiration

Actual evapotranspiration is determined by the potential evaporation, soil moisture, and vegetation/land cover specific parameters. In this study the moisture extraction function $f(\Theta)$ that modifies the potential crop coefficient is used (cf. Renger et al. 1974):

$$f(\Theta) = 0.2 + 2([\Theta - \Theta_W]/[\Theta_F - \Theta_W]) - 1.2([\Theta - \Theta_W]/[\Theta_F - \Theta_W])^2 \tag{23}$$

with:
Θ = soil moisture content (variable)
Θ_W = soil moisture content when soil is at wilting point
Θ_F = soil moisture content when soil is at field capacity

The crop coefficient (*KC*) varies intra-annually as given in Table 1 for all non-evergreen vegetation units, as water is mainly required by plants during photosynthesis. Divided into 10 time steps per day, the actual evapotranspiration calculates as

$$ET_A = ET_0 \times KC \times f(\Theta) \tag{24}$$

2.8 Interflow and groundwater recharge

Percolation II is developed by soil water content exceeding the field capacity. At the boundary of the soil with the subsoil (zone underneath the root zone) the percolation II is divided into interflow II (*WII*) and groundwater recharge (*GWR*) by comparing the permeability of the subsoil (*KG*) with the percolation II.

$$GWR = KG \qquad DPII > KG \tag{25}$$
$$WII = DPII - KG \qquad DPII > KG \tag{26}$$
$$GWR = DPII \qquad DPII \leq KG \tag{27}$$
$$WII = 0 \qquad DPII \leq KG \tag{28}$$

Precipitation, effective precipitation, potential evapotranspiration, real evapotranspiration, soil moisture content, groundwater recharge and interflow are the output parameters of the model at a daily resolution. Interflow summarises the surface runoff, interflow I and interflow II.

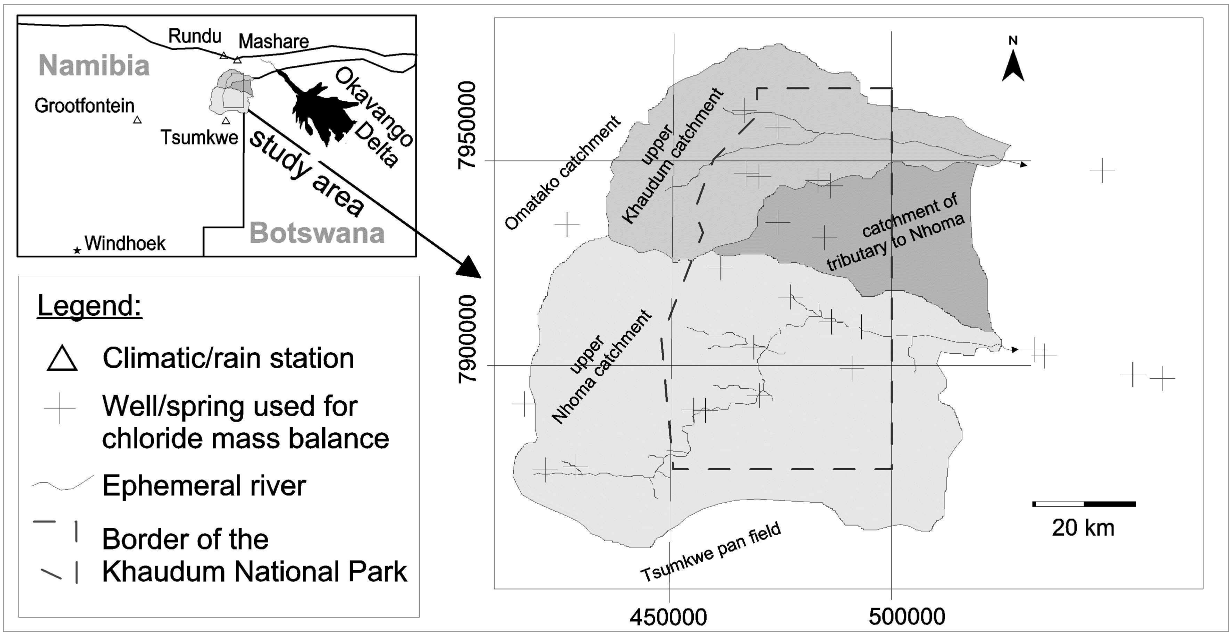

Figure 2: Location of the study area and Khaudum National Park.

3 Input data

3.1 Spatial input data

The study covers the area of the upper catchments of the Nhoma and Khaudum ephemeral rivers in the Khaudum National Park and adjacent land in north-eastern Namibia and north-western Botswana (412000E to 529000E and 7854000S to 7977000S (Fig. 2). The entire area is divided into cells each 500 by 500 m, forming a grid of 57564 boxes arranged as 246 rows by 234 columns and each grid point is identified by its georeferenced position in UTM 34S coordinates. The catchments are represented by a total of 39890 active cells.

Spatial input data required for the water balance model are topographic elevation, slopes and aspects, effective hydraulic conductivity at field capacity of the soil, plant available water content, interception storage, and saturated hydraulic conductivity of the subsoil. Spatial variations on these data are revealed by the use of published data on vegetation, soils and elevation in combination with detailed field work.

The study area can be subdivided into two major vegetation units according to Burke (2002): Eastern Paleo-drainage and Southern Panfield vegetation. As vegetation types are strongly related to topographic position and soil type, each of these units has been divided into several subunits based on a detailed vegetation study in the Khaudum National Park. Typical vegetation subunits on sand plains are woodlands dominated by Sandsyringe *Burkea africana* (subdominant *Pterocarpus angolensis*, *Guibourtia coleosperma*, *Terminalia sericea*), or by Zambezi Teak *Baikiaea plurijuga* (subdominant *Burkea africana*, *Terminalia sericea*). Dry river beds and pans are typically covered by grass only. Shrublands with dominant Acacia and Combretum species are constrained to shallow soils and the vicinity of hardrock outcrops. The six subunits used in this water balance model with their hydrologically relevant properties are summarised in Table 1. The distribution of the vegetation units in the Khaudum National Park are adopted from Wanke (2006) and projected into the adjacent areas by the use of a DEM and Landsat TM 7 imagery.

Dominant soils of the study area are ferralic arenosols, dystic regosols and eutric fluvisols (Mendelsohn et al. 2002). These soil types were recognised in the field and three textural classes derived. Subsequently grain size analyses have been performed. Field capacity and water content at wilting point for a unit meter depth of soil (uFC and uWP), and hydraulic conductivity at field capacity, are calculated using transfer functions from Saxton et al. (1986). However, the determination of water content from soil samples of the study area during the wet season revealed values significantly lower than those computed for the wilting point after Saxton et al. (1986). It is very likely that plants naturally adopted to the semiarid climate are able to extract water from the soil even at significantly lower matrix potential than the agricultural reference crops. Therefore measured residual water contents (uRWC) are used instead. Subtracting uRWC from uFC gives the plant available water content for a unit meter depth of soil (uAWC).

The plant available water content (AWC) is calculated by multiplying the uFC with the root depth for the relevant vegetation unit (Table 1). Effective rooting depths is set to 0.4 m for grasslands, 0.8 m for savannas and shrublands, and 1 m for woodlands, as these are the depths to which the largest part of root extends. According to Canadell et al. (1996) most of the root biomass occurs in depths of up to 0.5 m. However, maximum rooting depths in tropical grasslands and savannas exceed these values, clearly ranging from 1.5 to 68 m (Canadell et al. 1996). A factor only indirectly included in this hydrological model is the influence of "hydraulic lift" on the water balance. During the night deep roots take up water from deep soil layers and release it to shallow soil parts. During the next day this water is taken up and transpirated by the same plants and by others that do not have deep roots (Richards and Caldwell 1987; Caldwell and Richards 1989; Dawson, 1993). As this factor is not yet quantified, however, we have in this study used rooting depths that are reasonable from field observation and from the results of model calibration runs with different rooting depths. A variation of rooting depth with seasons is not included in the study, as all shrubs and trees in the study area are permanent. The dominant grass species such as *Cynodon dactylon*, *Eragrostis lehmanniana*, *E. trichophora*, *E. superba*, *Phragmites australis* and *Urochloa mosambicensis* are also permanent. The only annuals are some creepers and herbs that occur in negligible numbers.

The distribution of the topographic elevation in the study area is taken from SRTM data. The altitude ranges from 1009 to 1201 m above mean sea level with an area mean of 1104 m. Data are checked for accuracy against topographic maps of the study area. Slopes and aspects of the study area are derived using standard GIS techniques. The area is characterised as very flat with slopes ranging from 0 to 3.9% and an area mean of 0.33%.

3.2 Temporal input data

Temporal input data used in MODBIL are daily precipitation, minimum and maximum daily temperature and relative humidity at 14:00 hrs. The two climatic stations used in this study for minimum and maximum daily temperature and relative humidity are Grootfontein and Rundu (Fig. 2). During modelling performance it was found that using only one of these stations does not change modelling results because weather conditions are rather constant over the study area. Hence, data from the Grootfontein station only are used because this is an almost complete record. Using the Grootfontein data set only, a longer reliable observation period as modelling input was achieved.

The three relevant precipitation stations for this study are Tsumkwe, Rundu and Mashare (Fig. 2). These three stations are able to reproduce the general precipitation gradient over north-eastern Namibia. However, a major problem of precipitation regionalisation in drylands is the spottiness of single events. If three stations, each recording local rain events, are used in a general interpolation procedure, the local events are smoothed-out over the entire area leading to a precipitation regime that has more events, but in which each single event is of a lower precipitation amount. Thus, the precipitation regime revealed from such a standard interpolation does not mirror the actual conditions. In contrast, using only a single station reflects the typical temporal variations (frequencies and intensities) of precipitation well, but not precipitation gradients.

Therefore, virtual time series are produced for the two stations Mashare and Rundu, and used together with the real time series from Tsumkwe. To produce the virtual precipitation series, the total rain fall every month at Tsumkwe is compared with Mashare and Rundu respectively. Daily rain data from Tsumkwe are multiplied by the appropriate factor to produce virtual Mashare and virtual Rundu rain time series. The daily precipitation grids obtained do not, therefore, represent single stations and single days, but they mirror the long-term precipitation regime significantly better than standard interpolation procedures. Windspeed is set to a constant of 2 m s^{-1} (mean value for Rundu and Grootfontein) since time series for this parameter show large gaps.

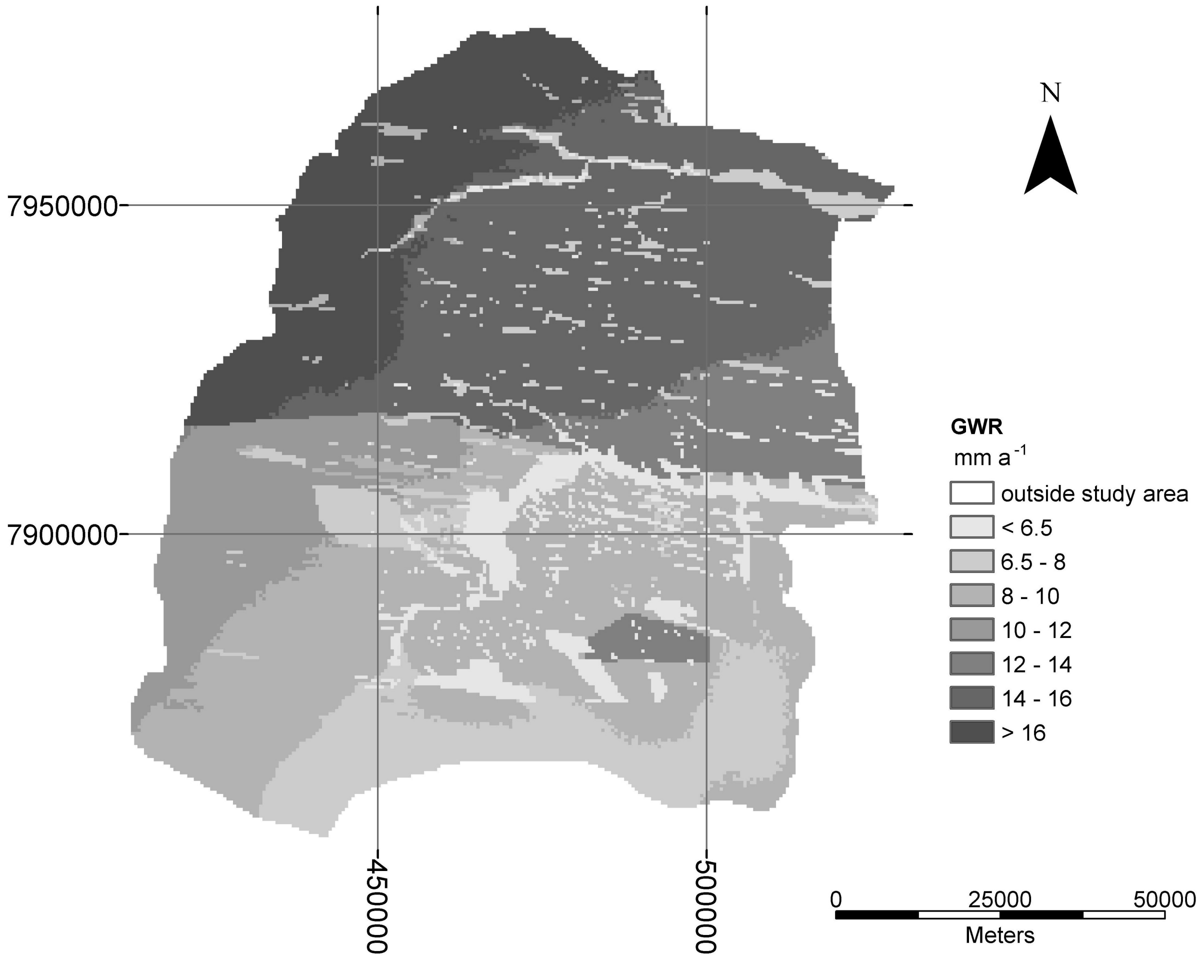

Figure 3: Spatial distribution of mean annual groundwater recharge for the upper Khaudum and Nhoma catchment in northeastern Namibia and northwestern Botswana. Model results for the time period 1st October 1982 - 30th September 2004.

4 Results and discussion

A mean annual groundwater recharge of 11.5 mm a^{-1} is calculated for the upper Khaudum and Nhoma catchments. This parameter ranges spatially from 0 to 17.5 mm a^{-1}. In general an increasing groundwater recharge can be observed from the south to the north (Fig. 3), which reflects the precipitation gradient. The pattern is modified by the influence of vegetation and soil. Highest recharge values occur in the *Burkea africana* savannah, which dominates the northern part of the study area. Relatively low recharge values are found in the *Acacia* shrubland, which dominates areas of relatively shallow soils in the southern part of the park, and pans in the northern part. No direct recharge is calculated for grasslands that cover parts of the ephemeral rivers and a few pans. However, interflow occurs almost exclusively in this unit ranging from 199 to 227 mm a^{-1} with a mean of 215.6 mm a^{-1}. Mean interflow for all other units is only 0.1 mm a^{-1} (Table 2). Real evapotranspiration also shows a significant difference between the grassland unit and all other units, with mean values of 240.9 and 442.6 mm a^{-1}, respectively.

Table 2: Mean values of the major components of the water balance for the modelling period 1st October 1982 - 30th September 2004 for the upper Nhoma and Khaudum catchments.

		Min	Max (mm a^{-1})	Mean	Number of cells
Precipitation	Study area	**423**	**474**	**450.5**	**39890**
ET real	Study area	**236**	**464**	**441.6**	**39890**
	Grasslands in ephemeral river	236	244	240.9	187
	Other units	420	464	442.6	39703
Interflow	Study area	**0**	**227**	**1.1**	**39890**
	Ephemeral river	199	227	215.6	187
	Ephemeral river Nhoma	199	224	206.9	112
	Ephemeral river Khaudum	217	227	221.4	75
	Other units	0	2	0.1	39703
Groundwater recharge	Study area	**0**	**17.5**	**11.5**	**39890**
	Nhoma catchment	4.8	17	10.3	29761
	Khaudum catchment	6.6	17.5	15.2	10129
	Mixed Savanna	6.9	12.2	9.0	17076
	Burkea africana Savanna	12.3	17.5	15.3	17959
	Acacia shrubland	5.1	8.9	6.6	4021
	Grassland	0	0	0	187
	Baikiaea plurijuga Woodland	7.6	9.9	8.6	347
	Terminalia prunioides Woodland	4.8	6.4	5.2	300

Mean annual recharge in the Khaudum catchment is greater than in the Nhoma catchment (Table 2). This reflects the precipitation gradient and the dominant soil and vegetation units. *Burkea africana* savannah has lower plant available water content than the mixed savannah and *Acacia* shrubland which is more common in the Nhoma catchment and thus leads more often to groundwater recharge. Simulated interflow developed in the ephemeral Khaudum river is also slightly higher than in the Nhoma. This is consistent with field observations: depressions in which water was collected are found more often in the Khaudum river. However, no flood events are recorded from either ephemeral river. Gradients are very low and runoff is collected locally in numerous pans in the river bed. One ephemeral/seasonal spring is known from the Khaudum river (opened by elephants a few years ago) which is most likely fed by interflow.

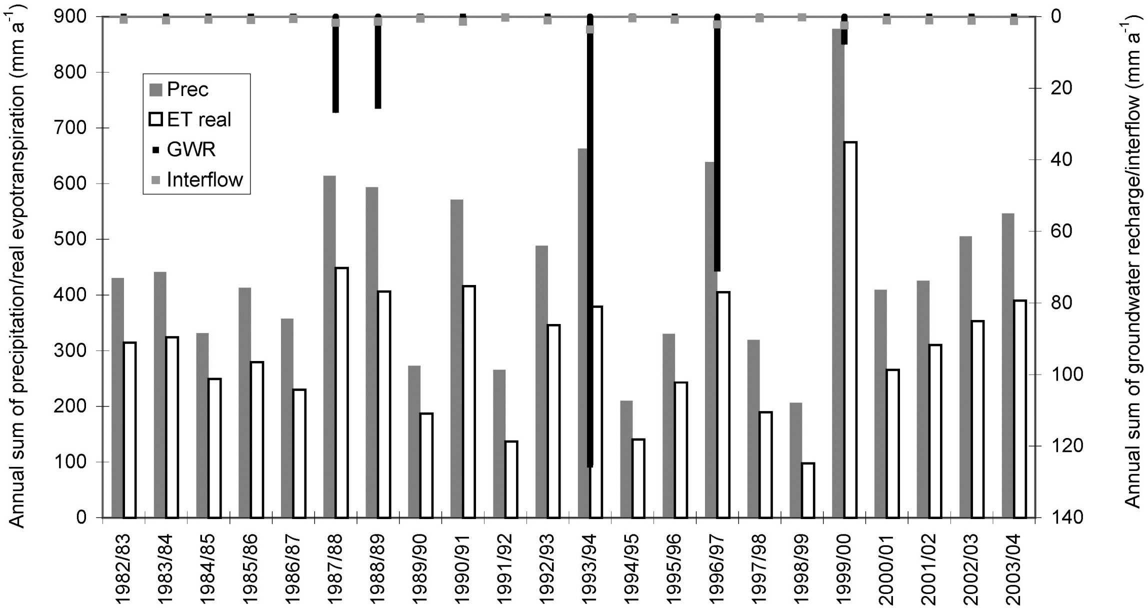

Figure 4: Modelled components of the water balance: Annual sums of precipitation, real evapotranspiration, groundwater recharge and interflow as area mean values for the study area.

Groundwater recharge occurs in only 5 out of 22 years during the modelling period, ranging form 6.9 to 125 mm a^{-1} (Fig. 4), or 0.8 to 18.9% of the total annual precipitation. Interflow, ranging from 0.2 to 3.6 mm a^{-1}, shows less variation as it occurs in every year, but interflow is also comparably high in the recharge years. As shown in Fig. 5 groundwater recharge has a high inter- and intra-annual variability. It occurs only during the second half of the season in years with extraordinarily high precipitation amounts. However, the total annual precipitation is not the only parameter that influences groundwater recharge. Fig. 6 indicates clearly that total precipitation is important, but in the case of the rainy season 1999/2000 which received a cumulative precipitation amount of 878 mm a^{-1}, only a relatively small amount of recharge is simulated (6.9 mm a^{-1}, 0.8%). In this case, a large part of the precipitation occurred early in the wet season and was interrupted by several dry periods that allowed much of the soil water to evapotranspirate. This becomes evident in the comparably high modelled real evapotranspiration (Fig. 4).

The most important years for groundwater recharge within the modelling period are 1987/88 (4.2% of the precipitation amount), 1988/89 (4.2%), 1993/94 (18.9%) and 1996/97(11%). It is observed for these years that a period of extensive rain occurred prior to the recharge events. For example, in 1993/94 recharge occurred from 4th - 23rd January as a consequence of a cumulative precipitation amount of 390 mm from 1st - 23rd January. Within this period, 16

Table 3: Comparison of groundwater (GW) recharge estimates for point data prepared with the chloride mass balance (CBM) and model recharge data.

Name	UTM East	UTM South	Sample year	Cl in GW (mg l^{-1})	Rain (mm a^{-1})	Cl in rain (mg l^{-1})	Cl deposition (mg m^{-2} a^{-1})	GW recharge CBM (mm a^{-1})	GW recharge model (mm a^{-1})
Samagaigai	415139.18	7889087.40	2000	30	438.2	0.6	315.5	10.5	
New Nhoma	419782.43	7873012.39	2000	95	404.6	0.6	291.3	3.1	
Xeidang	425018.37	7933168.75	1992	52	463.4	0.6	333.6	6.4	
Old Nhoma	426979.75	7873691.14	2000	11	397.6	0.6	286.3	26.5	
Close to Tsoanafontein	454424.03	7887309.93	Unknown	184	415.8	0.6	299.4	**1.6**	**5.6**
Tsoanafontein	456934.99	7888577.41	2005	257	415.8	0.6	299.4	**1.2**	**0**
Elandsvlakte	461291.33	7922455.01	2005	15	443.8	0.6	319.5	21.3	
WW33575	465789.71	7961043.09	1992	1115	459.2	0.55	303.1	0.3	
Near Burkea	466943.07	7945703.27	Unknown	18	453.6	0.55	299.4	**16.6**	**15.6**
Omuramba	469778.44	7903891.02	2005	54	431.2	0.55	284.6	5.3	
Soncana	469906.59	7892843.27	2005	49	420.0	0.55	277.2	**5.7**	**5.5**
Old Soncana	469957.32	7893134.36	1971	54	422.8	0.55	279.0	**5.2**	**5.7**
Burkea	469894.82	7945140.21	2005	15	453.6	0.55	299.4	20.0	
Khaudum	474104.17	7957121.71	2005	17	457.8	0.55	302.1	17.8	
Old Tsau	474184.74	7934131.88	Unknown	10	446.6	0.55	294.8	29.5	
Tsau	474513.81	7933820.68	2005	6	446.6	0.55	294.8	49.1	
Near Tari Kora	476822.94	7916861.65	Unknown	11	438.2	0.55	289.2	26.3	
Doringstraat	483401.16	7943816.21	2005	20	446.6	0.55	294.8	**14.7**	**15.3**
Old Leeupan	485291.19	7930072.46	Unknown	21	445.2	0.55	293.8	14.0	
Leeupan	485298.57	7930077.63	2005	65	445.2	0.55	293.8	4.5	
Old **Doringstraat**	486105.84	7943359.22	Unknown	22	446.6	0.55	294.8	**13.4**	**15.2**
Tari Kora	486391.43	7910798.42	2005	12	434.0	0.55	286.4	23.9	
Baikiaea	491180.66	7897907.20	2005	16	427.0	0.55	281.8	17.6	
Nhoma Boarder	493850.50	7907945.84	1972	220	429.8	0.5	257.9	1.2	
Nxaunxau I	534709.42	7902490.47	1984	205	428.4	0.5	257.0	1.3	
Nxaunxau II	536928.62	7900949.27	1983	93	425.6	0.5	255.4	2.7	
Xaudum	550941.96	7946619.67	1981	800	428.4	0.5	257.0	0.3	
Xaraxau I	557819.41	7895947.48	1988	47	421.4	0.5	252.8	5.4	
Xaraxau II	564802.71	7894971.59	1988	353	422.8	0.5	253.7	0.7	

rainy days occurred with daily rain amounts between 1.6 and 89 mm d^{-1}, and the last 7 days contributed 237 mm to the total.

The calculated mean groundwater recharge for the study area corresponds to 2.6% of the mean annual precipitation. This is in the same range as studies in southern Africa under similar climatic conditions confirm. Verhagen (1995), for example, obtained a recharge value of 1.8 to 3.3% by application of the CMB in Botswana (450 mm a^{-1} rain). Gieske (1992) obtained 2% groundwater recharge from the CMB and hydrograph interpretation in the Molepolole area in Botswana (492 mm a^{-1} precipitation), and Sloots and Wijnen (1990) calculated 1.2 - 2.5 % for the same area. Selaolo's (1998) results for the Letlhakeng-Botlhapatlou range up to 3.3%. Houston (1988) applied a water balance model in Zimbabwe and simulated 2% of the 500 mm a^{-1} precipitation as groundwater recharge. A recharge regionalisation by satellite images in combination with point results from the CMB for north-eastern Namibia (Klock, 2002) has also the same order of magnitude.

The mean interflow/runoff simulated in this study as 1.1 mm a^{-1} is a reasonable result for the Kalahari and it is consistent with observation from Külls (2000) in the Omatako catchment west of the study area (range 0.6 to 1.4 mm a^{-1}). In this study the CMB is used to verify the groundwater recharge results. Detailed descriptions of the method can be found in Edmunds et al. (1988), Edmunds and Gaye (1994) or Wanke (2005). In general it is used in the unsaturated zone, but can also be applied to relatively shallow groundwater samples. In that case the results represent an average recharge between the point where the water entered the saturated zone and the sampling point. We used 29 water samples (for locations see Fig. 2) to estimate the areas groundwater recharge rate as summarised in Table 3. Groundwater recharge from the water balance model is only given for wells with a groundwater level of 10 m below surface or less (bold letters in Table 3). Chloride data in groundwater were obtained from the Department of Water Affairs in Windhoek, the Division of Environmental Geology of Botswana and from own analyses. Rain amount is taken from the interpolation in MODBIL, chloride concentration in rain from Klock (2002) and dry deposition is assumed to contribute with 20 % to the total chloride deposition (Wanke 2005). A mean value of 11.9 mm a^{-1} is obtained which corresponds closely to the results from the water balance model (11.5 mm a^{-1}). In addition, groundwater recharge rates for wells with very shallow groundwater (less than 10 m for the Kalahari) are compared to point data from the simulation (bold samples in Table 3). A very close match is found for five out of these seven samples that confirm the spatial pattern of the simulation. However, deviations are higher for the samples from Tsoanafontein and close to Tsoanafontein. This probably results from the close proximity of different vegetation units in the neighbourhood of the well/spring, and thus the CMB recharge reflects the mixture of the grassland (0 mm a^{-1}) and Acacia shrubland (5.6 mm a^{-1}) zones in the catchment of the well/spring.

Monthly groundwater hydrographs from Tsumkwe are used for the temporal verification of the simulated recharge events. Hydrographs from Tsumkwe are from three abstraction wells, but production time series show large gaps so that quantitative recharge estimation is not possible on this basis. However, the hydrographs, which show increasing groundwater

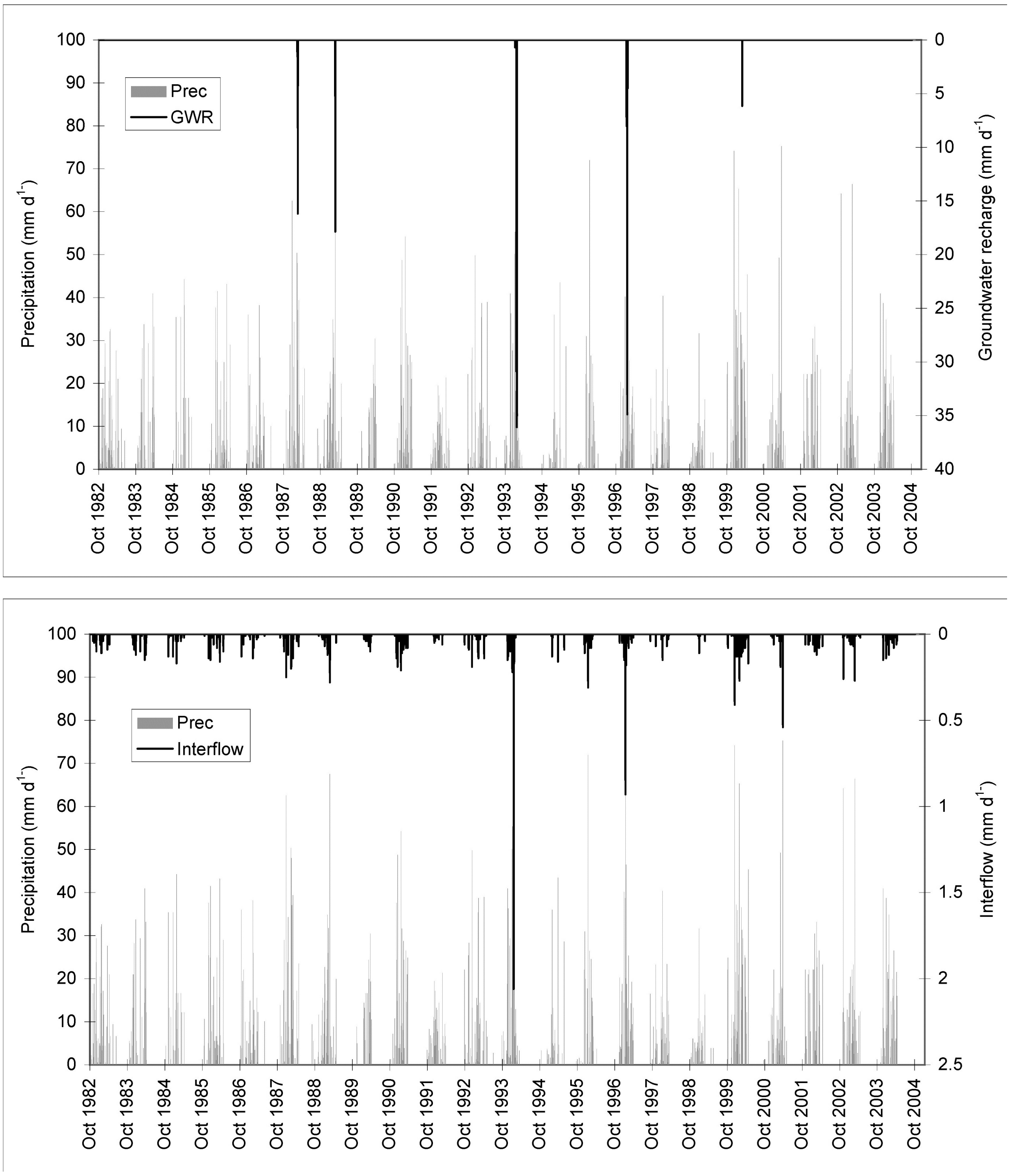

Figure 5: Modelled components of the water balance: Daily sums of groundwater recharge compared with precipitation (upper diagram) and daily interflow compared with precipitation (lower diagram) as area mean values for the study area.

levels during the relevant months, confirm all five simulated recharge events.

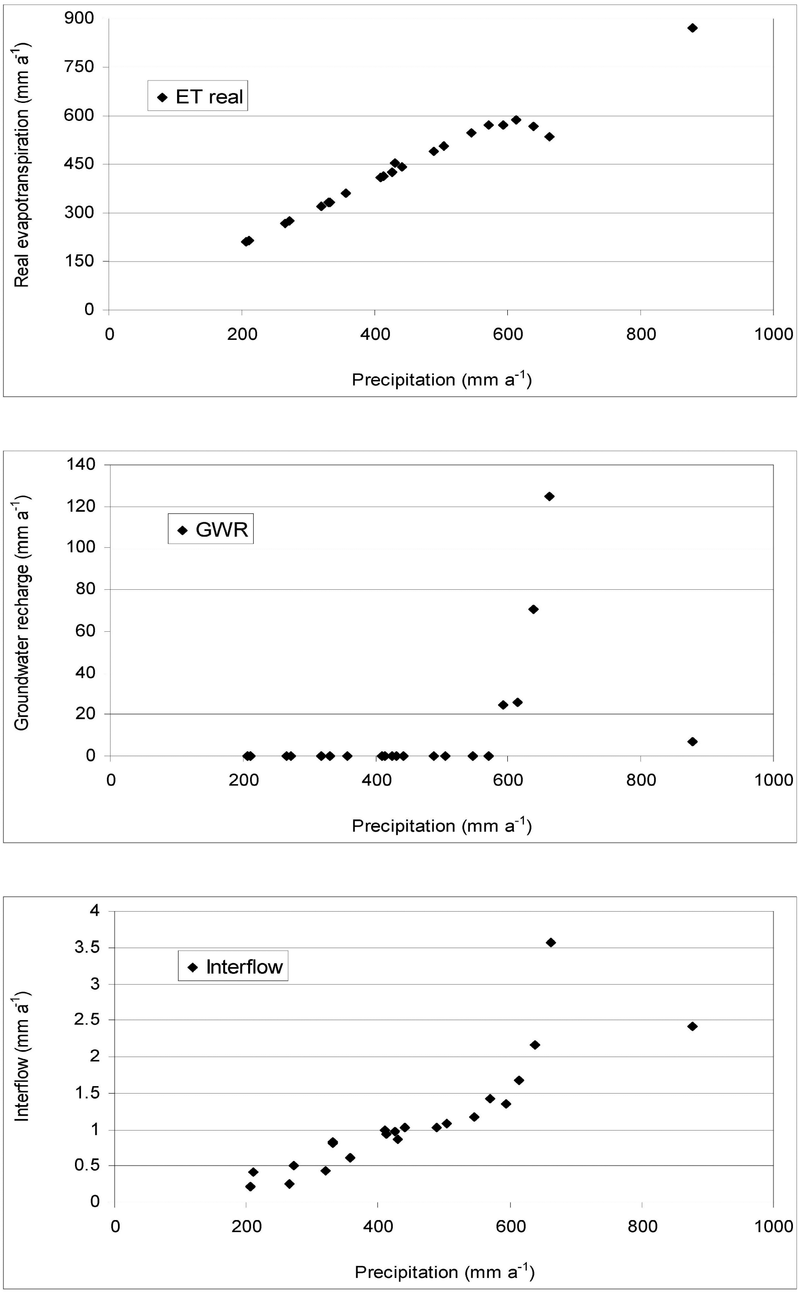

Figure 6: Plots of area mean values of annual sums of a) real evapotranspiration (upper diagram), b) groundwater recharge (middle diagram) and c) interflow (lower diagram) versus precipitation.

A factor that has not yet been included in this study is indirect recharge which likely occurs at least locally in the ephemeral rivers or pans. Isotopic studies by Külls (2000) indicate that between 1 and 3 % of the total recharge developed in the Omatako catchment results from local floods in the Kalahari. As this catchment is situated directly to the west of the study area and shows comparable surface properties and values for groundwater recharge and interflow, it is assumed that indirect groundwater recharge in the dry rivers is also of a comparable amount. Using this estimate, an area mean of 0.35 mm a^{-1} of indirect recharge would be added to the total groundwater recharge in the upper Khaudum and Nhoma catchments. Selaolo (1998) found a maximum indirect recharge of 30 mm a^{-1} under a pan in the Kalahari of Botswana. As pans and ephemeral rivers cover only 0.47 % of the study area (Table 1), an indirect recharge with this maximum value calculates as an area mean of only 0.14 mm a^{-1}. However, the error of the water balance model is assumed to be in the same order of magnitude as the indirect recharge.

5 Conclusions

This study shows that groundwater recharge in the upper Khaudum and Nhoma catchment has a high inter- and intra-annual variability. It occurs only during five of the 22 modelled years. These 5 years received extraordinarily high precipitation amounts in a relatively short period prior to the recharge events. As recharge occurs only on a few days it underlines the principle that daily climatic input data are the minimum required for water balance modelling in drylands.

Altogether a mean annual area groundwater recharge of 11.5 mm a^{-1} is calculated, but spatial variation between 0 and 17.5 mm a^{-1} occurs according to the variability of vegetation, soil and geomorphology. Inaccuracies can appear especially due to the uncertain distribution of root depth. As this parameter was assessed by model calibration, and almost no reliable published data can be found for natural vegetation units in the semiarid environment, further research is needed. This also points out the importance of model verification which is done in this study by the application of the chloride mass balance method and simple groundwater hydrographs. Further confirmation of the simulation results are found through a literature study on groundwater recharge and surface runoff in the southern African region.

As water balance modelling for the Kalahari is shown in this study to be reliable, this method can also be applied to more challenging questions of future water resource planning. For instance, a combination with climatic or land use prediction models would allow dynamic estimates for the development of the water resource.

Acknowlegements

The authors wish to thank the Ministry of Environment and Tourism in Namibia for logistic support of the field work. Dries Alberts (MET) is especially thanked for providing us with internal data. The Weather Bureau of Namibia is kindly acknowledged for the supply of climatic data. The Department of Water Affairs in Namibia and the Division of Environmental Geology in Botswana are thanked for adding hydrochemical information to our database. The HWP (Hochschulwissenschaftliches Programm der Universität Würzburg), DAAD (Deutscher Akademischer Austausch Dienst) and the DFG (Deutsche Forschungsgemeinschaft) are acknowledged for funding parts of the project. Further thanks go to the reviewers of this manuscript for the constructive comments that helped to improve the manuscript.

References

[1] Alemawa BF, Chaoka, TR. A continental scale water balance model: a GIS-approach for Southern Africa. *Physics and Chemistry of the Earth* 28, 957-966 (2003)

[2] Allen RG, Pereira LS, Raes D, Smith M. *Crop evapotranspiration: guidelines for computing crop water requirements*. Irrigation and Drainage Paper 56. FAO, Rome, p. 300 (1998)

[3] Beekman HE, Selaolo ET, Nijsten G-J. Groundwater recharge at the fringe of the Kalahari - The Letlhakeng-Botlhapatou area. *Botswana Journal Earth Science* 3, 19-23 (1996)

[4] Burke A. Present vegetation in the Kavango region. *Journal Namibia Wissenschaftliche Gesellschaft / Namibia Scientific Society* 50, 133 145 (2002)

[5] Brunner P, Bauer P, Eugster M, Kinzelbach W. Using remote sensing to regionalize local precipitation recharge rates obtained from the chloride method. *Journal of Hydrology* 294, 241-250 (2004)

[6] Caldwell MM, Richards JH. Hydraulic lift: water efflux from upper roots improves effectiveness of water uptake by deep roots. *Oecologia* 79, 1-5 (1989)

[7] Canadell J, Jackson RB, Ehleringer JR, Mooney HA, Sala OE, Schulz E-D. Maximum rooting depth of vegetation types at the global scale. *Oecologia* 108, 583-595 (1996)

[8] Chidumayo EN. Climate and phenology of savanna vegetation in southern Africa. *Journal of Vegetation Science* 12, 347-354 (2001)

[9] Dawson TE. Hydraulic lift and water use by plants: implication for water balance, performance and plant-plant interaction. *Oecologia* 95, 565-574 (1993)

[10] Edmunds WM, Gaye CB. Estimating the spatial variability of groundwater recharge in the Sahel using chloride. *Journal of Hydrology* 156, 47-59 (1994)

[11] Edmunds WM, Darling WG, Kinniburgh DG. Solute profile techniques for recharge estimation in semi-arid and arid terrain. In: Simmers, I. (Ed.) *Estimation of natural groundwater recharge*, pp. 313-322. NATO ASI Series C 222. Reidle, Dordrecht (1988)

[12] Gieske A. *Dynamics of groundwater recharge - a case study in semi-arid eastern Botswana*. Ph.D. thesis, Vrije Universiteit Amsterdam (1992)

[13] Hendrickx JMH, Walker GR. Recharge from precipitation. In: Simmers, I. (Ed.) *Recharge of phreatic aquifers in (semi-)arid areas*, pp. 19-111. International Contributions to Hydrogeology, vol. 19. AA Balkema, Rotterdam (1997)

[14] Houston J. Rainfall-runoff-recharge relationship in the basement rocks of Zimbabwe. In: Simmers, I. (Ed.) *Estimation of natural groundwater recharge*, pp. 349-366. NATO ASI Series C 222. Reidle, Dordrecht (1988)

[15] Klock H. Hydrogeology of the Kalahari in north-eastern Namibia with special emphasis on groundwater recharge, flow modelling and hydrochemistry. *Hydrogeologie und Umwelt* 31, 1-196 (2002)

[16] Külls C. Groundwater of the North-Western Kalahari, Namibia Estimation of recharge and quantification of the flow system. *Hydrogeologie und Umwelt* 28, 1-165 (2000)

[17] Lerner DN, Issar AS, Simmers I. Groundwater recharge a guide to understanding and estimating natural recharge. *International contributions to Hydrogeology*, vol 8. Heinz Heise Verlag, Hannover (1990)

[18] Mendelsohn J, Jarvis A, Roberts C, Robertson T. *Atlas of Namibia: A portrait of the land and its people*. David Philip Publishers, Cape Town (2002)

[19] Monteith JL. Evaporation and environment. In: *Proceedings of the Symposium of the Society for Experimental Biology* 19, 205-234. Cambridge University Press (1965)

[20] Renger M, Strebel O, Giesel W. Beurteilung bodenkundlicher, kulturtechnischer und hydrologischer Fragen mit Hilfe von klimatischer Wasserbilanz und bodenphysikalischen Kennwerten. *Zeitschrift Kulturtechnik Flurbereinigung* 15, 148-160 (1974)

[21] Richards JH, Caldwell MM. Hydraulic lift: substantial noctural water transport between soil layers by Artemisia tridentata roots. *Oecologia* 73, 486-489 (1987)

[22] Rushton KR, Eilers VHM, Carter RC. Improved soil moisture balance methodology for recharge estimation. *Journal of Hydrology* 318, 379399 (2006)

[23] Saxton KE, Rawls WJ, Romberger JS, Papendick RI. Estimating generalized soil-water characteristics from texture. *Soil Science Society of America Journal* 50, 1031-1036 (1986)

[24] Scanlon BR, Cook PG (Eds.). Theme Issue: Groundwater recharge. *Hydrogeology Journal* 10, p. 237 (2002)

[25] Selaolo ET. *Tracer studies and groundwater recharge assessment in the eastern fringe of the Botswana Kalahari: the Letlhakeng - Botlhapatlou Area*. Ph.D. thesis, Vrije Universiteit Amsterdam (1998)

[26] Selaolo ET, Beekman HE, Gieske ASM , De Vries JJ. Multiple tracer profiling in BotswanaGRES findings. In: Xu Y & Beekman HE (eds.): *Groundwater Recharge Estimation in Southern Africa*, UNESCO IHP Series No. 64: 33-50 (1996)

[27] Simmers I (Ed.). Recharge of Phreatic Aquifers in (Semi-) Arid Areas. *International Contributions to Hydrogeology*, vol. 19. AA Balkema, Rotterdam, p. 277 (1997)

[28] Sponagel H. Zur Bestimmung der realen Evapotranspiration landwirtschaftlicher Kulturpflanzen. *Geologisches Jahrbuch* F 9, 3-87 (1980)

[29] Sloots RR, Wijnen MM. *Groundwater recharge to a fractured aquifer in S-E Botswana. Results of a survey of the Molepolole-East wellfield*. M. Sc. thesis, Vrije Universiteit Amsterdam (1990)

[30] Stone AEC, Edmunds WM. Sand, salt and water in the Stampriet Basin, Namibia: Calculating unsaturated zone (Kalahari dunefield) recharge unsing the chloride mass balance approach. *Water SA* 38, 367 378 (2012)

[31] Udluft P, Dünkeloh A. *MODBIL A numerical water balance model*. Unpubl. program and manual. Vers. 4.7 (December 2005), Würzburg/Germany (2005)

[32] Verhagen BT. Semiarid zone groundwater mineralization processes as revealed by environmental isotope studies. In Adar EM, Leibundgut C (Eds), *Application of tracers in arid zone hydrolgy*, pp. 245-266. IAHS Publ. 232 (1995)

[33] Wanke A. *A Profile of Khaudum National Park (Namibia) with emphasis on the physical environment, woody vegetation, and water*. M. Phil. thesis, University of Pretoria (2006)

[34] Wanke H. Abschätzung der Grundwasserneubildung in Namibia mittels der Chlorid-Bilanz-Methode: Ist die trockene Deposition vernachlässigbar? *Hydrogeologie und Umwelt* 33 (10): 1-14 (2005)

[35] Wanke H, Dünkeloh A, Udluft P. Groundwater recharge assessment for the Kalahari catchment of northeastern Namibia and northwestern Botswana with a large scale water balance model. *Water Resources Management* 22, 1143-1158 (2008)